https://doi.org/10.3311/PPci.37653

Periodica Polytechnica Civil Engineering, 69(2), pp. 519–528, 2025

Rock Mass Characterization and Non-destructive In-situ Testing of a Rock-cut Tomb: Theban Necropolis (Egypt)

Tamás Zomborácz[1*], Gábor Somodi[1], Sayed El Qurany[2], Ákos Török[1]

[1] Department of Engineering Geology and Geotechnics, Faculty of Civil Engineering, Budapest University of Technology and Economics, Műegyetem rkp. 3., H-1111 Budapest, Hungary
[2] Ministry of Tourism and Antiquities, El Adel Abou Bakr St., Zamalek head office 3, Zamalek, 11517 Cairo, Egypt
[*] Corresponding author, e-mail: zomboracztamas@edu.bme.hu

Received: 11 June 2024, Accepted: 10 December 2024, Published online: 10 February 2025

Abstract

The current study describes the engineering geological properties of a rock-cut tomb that is located near Luxor, forming a part of the Theban necropolis in Egypt. The studied Theban Tomb no. 25 (TT 25) was excavated during the New Kingdom and served as a funeral site. The host limestone belongs to the Late Paleocene Tarawan Chalk Formation. The site investigations included the detection of the joint system, the measurements of relative humidity and temperature cycles, and moisture content. The rock mass parameters were also outlined considering the strength (obtained from Schmidt hammer rebounds) and the orientation and frequency of joints. Five joint sets were identified: three sub-vertical and one bedding-controlled sub-horizontal. The results of temperature, relative humidity, and moisture content measurements support the observations, namely that salts accumulate at the sloping passage and burial chamber, where higher humidity provokes salt efflorescence.

Keywords

limestone, joint system, relative humidity, temperature, new kingdom

1 Introduction

Engineering geological research is essential in preserving subsurface openings, such as caves, cellars or even tombs. Previous studies focused on the material testing and stability calculations of such systems, and examples are known from Spain [1], form Italy [2], Hungary [3–5], and Korea [6]. Focusing on the study area of Egypt, the stability of selected tombs was also analyzed [7–10]. Before our work, we studied Aubry et al. [11–13], Dupuis et al. [14], Ziegler et al. [10] for creating a research plan and a complete engineering geological approach. Environmental factors and micro-climatic conditions also have an important role in the long-term preservation of such subsurface systems [15, 16].

By understanding the geological setting, assessing rock mass quality, and identifying potential hazards of failure, researchers can develop conservation strategies. The integration of traditional field studies and in-situ measurements ensures a detailed analysis to handle these precious cultural treasures for future generations with care. The collaboration between geologists, engineers, conservators, and archaeologists is crucial to ensure the long-term preservation of the tombs of this cultural heritage site.

The current study presents the engineering geological research of the Ramesside rock-cut tomb of Amenemhab (TT 25) situated in the northern Asasif area within the Theban necropolis. Being used as a burial site for almost two millennia, the cemeteries of el-Asasif are home to numerous noble tombs constructed for high dignitaries and their families. The geography and the geology of the study area were summarized by previous authors [11–14], and the studied tomb's geometry, architectural components, and mural decoration are mostly known from the surveys of Porter and Moss [17] and Kampp [18]. With the joint system characterization and measurements of relative humidity and temperature, as well as the moisture content of selected walls, it is possible to provide data for the long-term behavior of this tomb. The critical factors contributing to the damage of the subsurface system, such as fractures and salt efflorescence, are discussed using engineering geological and environmental considerations.

2 Geography and geological setting

The Plain of el-Asasif lies at the base of the Theban Mountain within the Theban necropolis on the west bank

Cite this article as: Zomborácz, T., Somodi, G., El Qurany, S., Török, Á. "Rock Mass Characterization and Non-destructive In-situ Testing of a Rock-cut Tomb: Theban Necropolis (Egypt)", Periodica Polytechnica Civil Engineering, 69(2), pp. 519–528, 2025. https://doi.org/10.3311/PPci.37653

of the River Nile, opposite the modern city of Luxor in Upper Egypt. The Asasif area encompasses two regions, both located at the mouth of valleys leading to the west: 1) the northern plain, i.e., North Asasif (which el-Asasif is commonly associated with), situated east of Deir el-Bahari, between Dra' Abu el-Naga' and the hills of el-Khokha and Sheikh Abd el-Qurna, and 2) the southern plain, i.e., South Asasif, stretching south of the southern slope of Sheikh Abd el-Qurna (Figs. 1 and 2).

The New Kingdom tomb of Amenemhab (TT 25) is located within the cemeteries of the northern plain which is home to numerous private rock-cut tombs dating from

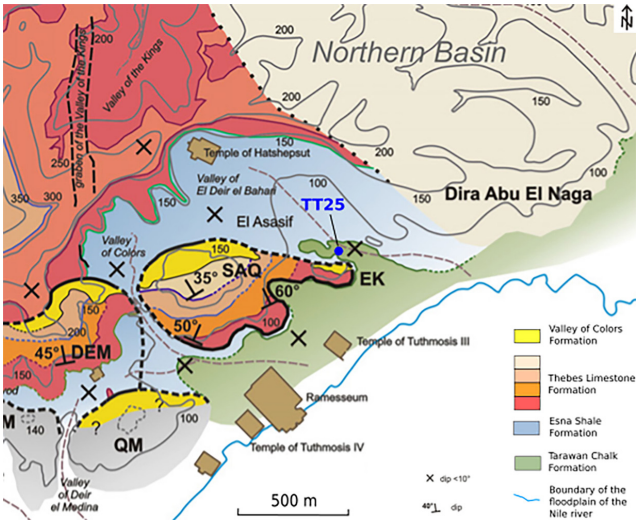

Fig. 1 Geological setting of the surrounding of the Asasif area in the Theban necropolis. The location of TT 25 is marked on the map. (after Dupuis et al.) [14]

Fig. 2 Aerial photo of the northern region of the Theban necropolis photographed from the east (photo by Gy. Csáki, 1989). The position of TT 25 is marked by a red cross. DAN: Dra' Abu el-Naga', DEB: Deir el-Bahari, EK: el-Khokha, NA: North Asasif, SA: South Asasif, SAQ: Sheikh Abd el-Qurna, VOC: Valley of the Colors, VOK: Valley of the Kings

the Middle Kingdom to the Ptolemaic period. Although TT 25 is generally attributed to el-Asasif, in a geomorphological sense it belongs to the Hill of el-Khokha, as it was cut into the base of the neighboring hillock's northern flank, at the southern boundary of North Asasif.

The Theban necropolis lies at the edge of the Western Desert, generally referred to as the Theban Mountain [11]. The landscape is dominated by sub-vertical cliffs that delineate the easternmost edge of the Theban Plateau, and a group of low hills, i.e., the Theban hills [14] lining up in front of the prominent cliffs of the plateau. The bedrock of the Theban Mountain is composed of a ca. 550 m thick upper Paleocene-lower Eocene succession that consists of three main sedimentary units, from base to top: the Tarawan Chalk Formation, the Esna Shale Formation, and the Thebes Limestone Formation [12].

The Plain of el-Asasif is composed of the sub-horizontally stratified Esna Shale Formation, a heterogenous succession of shales that outcrops at a large continuous area at the foot of the Theban cliffs. Esna Shales form the northern and southern plains of el-Asasif, as well as the floor of the Amphitheatre of Deir el-Bahari and the Valley of the Colors in between them, and extend all the way to the Valley of Deir el-Medina [13] (Fig. 1). North Asasif is formed by very low hills (referred to as the Hills of el-Asasif by Aubry et al.) [13] that are composed of the lowermost member (Hanadi) of the Esna Shale Formation and the underlying Tarawan Chalk Formation [12]. In the northern Asasif area, outcrops of the Tarawan Chalk occur at the south-eastern boundary of the plain, at the foot of the neighboring el-Khokha hill. The homogenous lithology consists of a soft, white, fine-grained limestone with isolated flint layers, although its carbonate content decreases as it passes gradually into the overlying Hanadi Member of the Esna Shale Formation [13].

In the Hills of el-Asasif, tombs were cut into the Tarawan Chalk Formation, thus, it is the host lithology of the subject of this paper (TT 25), as well.

3 Description of the tomb

The studied Theban Tomb no. 25 (TT 25) is located within the cemeteries of el-Asasif, quarried into the upper Paleocene Tarawan Chalk Formation at the base of el-Khokha hill's northern slope, at the southern boundary of the northern Asasif area. The tomb's entrance opens from a large courtyard, along with several other tombs of similar period (Figs. 3 and 4). The construction of TT 25 is dated to the 19th Dynasty of the New Kingdom, the reign

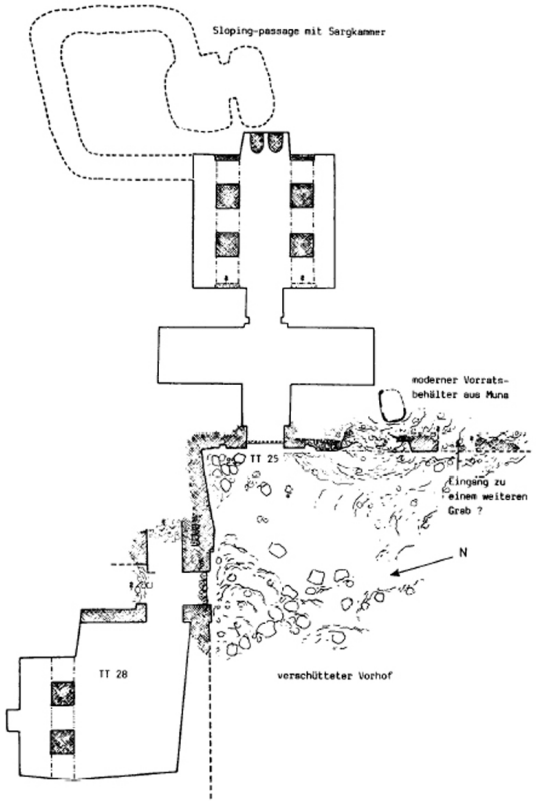

Fig. 3 The ground plan of TT 25 and its northern neighbor, TT 28 by Kampp [18]. Both tombs open from a large courtyard, along with several other tombs of similar period. Note that at the time of Kampp's survey the floor of the courtyard was buried under debris, and the design and the access to the sloping passage in TT 25 were not drawn by the author but taken from another article and inserted into the ground plan (Kampp, 212) [18]

Fig. 4 The north-eastern corner of the large courtyard where the entrance of TT 25 (in the middle) opens from. Note the entrance of the two neighboring tombs to the left (TT 28) and to the right (unnumbered)

of Ramesses II (13th c. BCE) [17, 18]. The tomb's owner, Amenemhab was the "First prophet of Khons" [17].

As no architectural components belonging to TT 25 remained in the courtyard, the original extent of the tomb's forecourt is uncertain. The tomb's interior consists of two cult rooms, a sloping passage (i.e., a narrow sloping corridor leading to the chambers), a burial chamber and its fore-chamber (Fig. 3). The two cult rooms were arranged according to the traditional T-shaped ground plan following the post-Amarna canon of mortuary monuments that can be observed in the vicinity of the area [19]. The first (western) cult room is a transverse hall (Fig. 5), whilst the second (eastern) cult room is a square-based pillared hall divided into three colonnades by two lines of columns (Fig. 6). This type of the T-shaped Theban tombs (classified as '*Type VIb*' by Kampp) [18] can be found in a similar form not too far away on the eastern slope of the el-Khokha hill (TT 49, TT 373, and –354–) [18].

Painted decoration only remained in the transverse hall, and due to the lack of traces of paint in the second room, it can be assumed that the mural decoration of the tomb was only partly finished. (For detailed description of the painted scenes (Porter and Moss [17]), 42. In order to

Fig. 5 Southern half of the transverse hall (first cult room). The entrance of the tomb is on the right, and the door leading to the second cult room is on the left

Fig. 6 The pillared hall (second cult room) towards the east. The unfinished statue of the deceased (and his family) carved into the rock can be found in the niche on the central axis of the tomb

provide an even surface for the wall paintings, the uneven sidewalls and the ceiling were plastered. For this purpose, earth plaster strengthened with fibrous organic material was used. In the pillared hall, two shafts of secondary burials are present. At the eastern end of the room, the unfinished statue of the deceased (and presumably his wife) carved into the rock can be found in a niche (Fig. 6). The sloping passage opens from the north-eastern corner of the pillared hall. Both the sloping passage and the burial chamber are undecorated (Fig. 7).

4 Methodology

4.1 Temperature and relative humidity monitoring

With the aim of monitoring temperature and relative humidity changes during daily and annual cycles both inside and outside the tomb, environmental data collection was started in TT 25 in February 2024. Data recording is being carried out with temerature and humidity data logger devices (Table 1) placed at three selected sampling points (Table 2, Fig. 8). In order to collect representative data, sampling must be continuous for at least a one-year period.

Fig. 7 The fore-chamber photographed from the ending of the sloping passage. On the left, a flight of stairs leads to the burial chamber

Table 1 Technical details of the temperature and humidity data logger device used for environmental data collection in TT 25

Data logger technical details	
Manufacturer	Steinberg Systems
Model	SBS-DL-123D
Temperature measurement range [°C]	–35÷80
Accuracy of temperature measurement [°C]	±0.3
Humidity measurement range [%]	0÷100
Accuracy of humidity measurement [%]	±3

Table 2 Details of temperature and humidity data recording in TT 25

Device no.	Measuring location	Sampling interval	Starting date
DL-10	burial chamber, W sidewall	2 h	18.02.2024
DL-11	room II, niche	2 h	18.02.2024
DL-12	façade, above entrance	2 h	18.02.2024

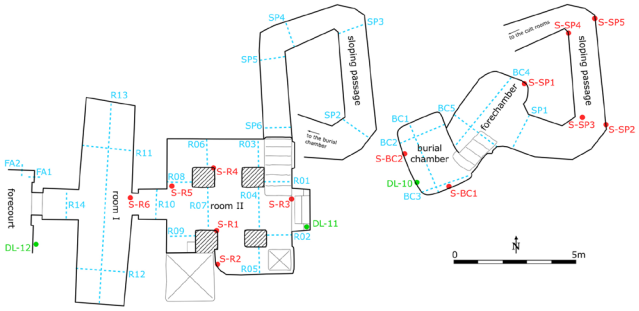

Fig. 8 The location of sampling points and profiles on the schematic ground plan of TT 25. *Blue*: moisture profiles (BC1–3, SP1–6, R01–14, FA1–2); *red*: Schmidt hammer test areas (S-BC1–2, S-SP1–5, S-R1–6); *green*: T & RH data logger sampling points (DL-10–12)

4.2 Surface moisture content measuring

In order to define the moisture content of the rock surfaces in the tomb's spaces, moisture measurements were carried out with a pinless moisture meter along vertical and horizontal profiles both in the inner spaces and on the façade wall (Table 3, Fig. 8).

4.3 Joint characterization and field observation

In order to get basic engineering geological parameters for the rock environment of the tomb, we use geotechnical mapping. It begins with defining and separating joint sets, which means that joints with the same orientation were classified into a joint set. During mapping type and thickness of infilling, surface roughness, length and mean spacing of joint sets were defined according to Bieniawski [20], Barton and Choubey [21] and Barton [22]. Orientation was measured with original compass and mobile applications. Average distance and length were measured with a simple geodetic tool. Joint orientation data were analyzed using Dips from the Rocscience software suite [23].

Table 3 Distribution of the measured moisture profiles in TT 25

Measuring location	No. of measured profiles
burial chamber	3
fore-chamber	2
sloping passage	6
room II	10
room I	4
façade	2

During description of joints we also carried out salt crystal observation. It needed detailed measurement of crystal height and defined crystal distribution along the tomb walls and ceilings.

4.4 Schmidt hammer

The Schmidt hammer rebound hardness test is a simple and non-destructive test that was originally developed for a quick measurement of uniaxial compressive strength (UCS), and later was extended to estimate the hardness and strength of rocks. Several researchers have proposed various empirical equations for calculating UCS from R (rebound number). They have found that Schmidt hardness and the UCS are closely related. Proper relationships between Schmidt hardness and UCS are part of the standard methods for the Schmidt hammer test in rocks that have been prepared by International Society for Rock Mechanics [24] and ASTM [25].

5 Results

5.1 Temperature and relative humidity monitoring

Measurement data was first downloaded from all three measuring points after an 18-day test period. Therefore, current results only show temperature, relative humidity (RH) and dew point (DP) changes during daily cycles from 18th February to 7th March 2024, and thus, should be considered preliminary results only. However, these measurements provide a good background to understand the differences in the temperature and RH and DP in the burial chamber, in the room and at the entrance zone (façade) (Fig. 9).

The mean values of T, RH and DP as well as the maximum, minimum, average values and standard deviations are given in Table 4.

Field observation of salt crystals resulted in a sophisticated view of distribution patterns along the walls. We can conclude that these crystals are vast amounts of gypsum. There is no evidence for these gypsum in Room I or Room II and they are missing from the ceiling of the uppermost part of the Sloping passage. However, from the first turn of the Sloping passage the amount of the crystals

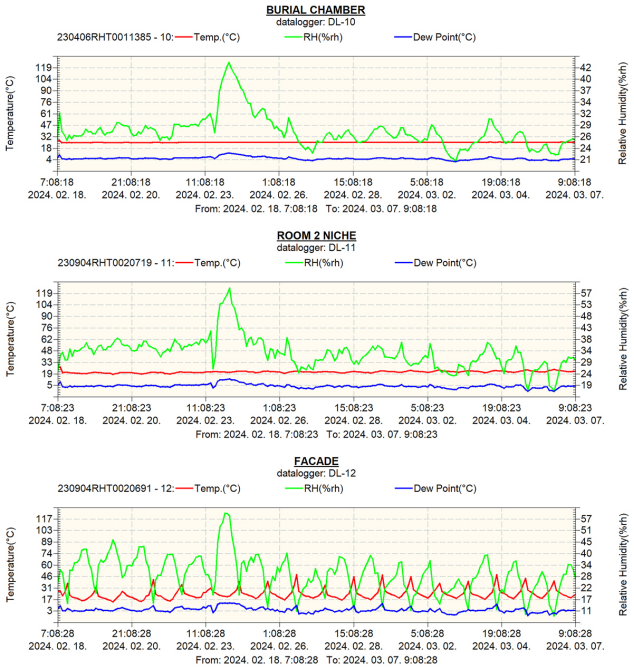

Fig. 9 Temperature, humidity and dew point changes in the burial chamber, room II, and façade during the 18-day test period

is decreasing rapidly, primarily on the walls after the second turn it becomes widely distributed along the whole route and the size of the crystals are getting larger, up to 5 cm. In the Fore Chamber and the Burial Chamber gypsums covered almost the whole wall and ceilings, the sizes reaching 5–10 cm very frequently.

5.2 Surface moisture content

As for the wall moisture content, we can say that three different distributions are found in the chamber and its surroundings. In the vestibule, the wall moisture content decreases from the bottom up, in chamber two it increases from the bottom up, and in the burial chamber the moisture content is roughly the same without trends or tendency (Fig. 10).

5.3 Joint patterns

The distribution of joint and fracture orientations shows different patterns in the different levels of TT 25. The burial chamber has a limited distribution of joint orientations,

Table 4 Technical details of the temperature and humidity data logger device used for environmental data collection in TT 25

	Burial chamber (DL-10)				Room II niche (DL-11)				Facade (DL-12)			
	Min.	Max.	Avg.	St.Dev.	Min.	Max.	Avg.	St.Dev.	Min.	Max.	Avg.	St.Dev.
Temperature (°C)	24.9	27.7	25.3	0.3	18.9	27.9	21.7	1.2	14.1	47.9	24.1	6.4
RH (%rh)	20.8	43.4	27.6	3.7	16.9	59.5	32.6	6.3	8.5	59.8	29.1	9.2
Dew point (°C)	1.3	12.0	5.1	1.8	–2.3	13.0	4.3	2.4	–3.0	13.0	4.1	3.1

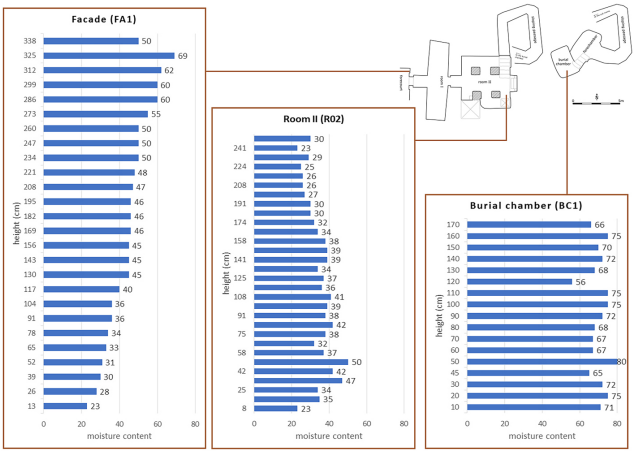

Fig. 10 Vertical moisture profiles at the entrance (Façade), in the second cult room (Room II), and in the Burial Chamber

which mostly defines the direction of the chamber walls, NNW-SSE dip directions and almost E-W direction of walls (Fig. 11 (b)). On the contrary, measured joints and fractures of the Sloping passage have a wide range of orientations with at least four different joint sets and several random joints (Fig. 11 (d)). In Room I and II show similarity with the Burial chamber, although the walls of the rooms have almost exactly E-W direction. However, the layer dip of Tarawan Chalk only appears on Fig. 11 (c) with 12/215 dip and dip direction. All fractures of TT25 are shown in Fig. 11 (a), and according to this figure we can observe four main joint sets beside the layer dip.

The results of engineering mapping, with the most characteristic joint sets and its parameters, are presented in Table 5, according to the result of orientation analysis it presents five different fracture sets (J1-J5). The most homogenous parameters are connected to infilling type and thickness, which is a maximum of 5 mm thick calcite. Besides, most apertures are closed or slightly opened. The average joint distances in one set are moderately jointed, closely and widely jointed. Sedimentary layers are hard to observe and for this reason there is no obvious data for distance between layer boundaries. The roughness of joint surfaces is mostly undulating smooth, which can be connected to Tarawan Chalk joint pattern with conchoidal type surfaces.

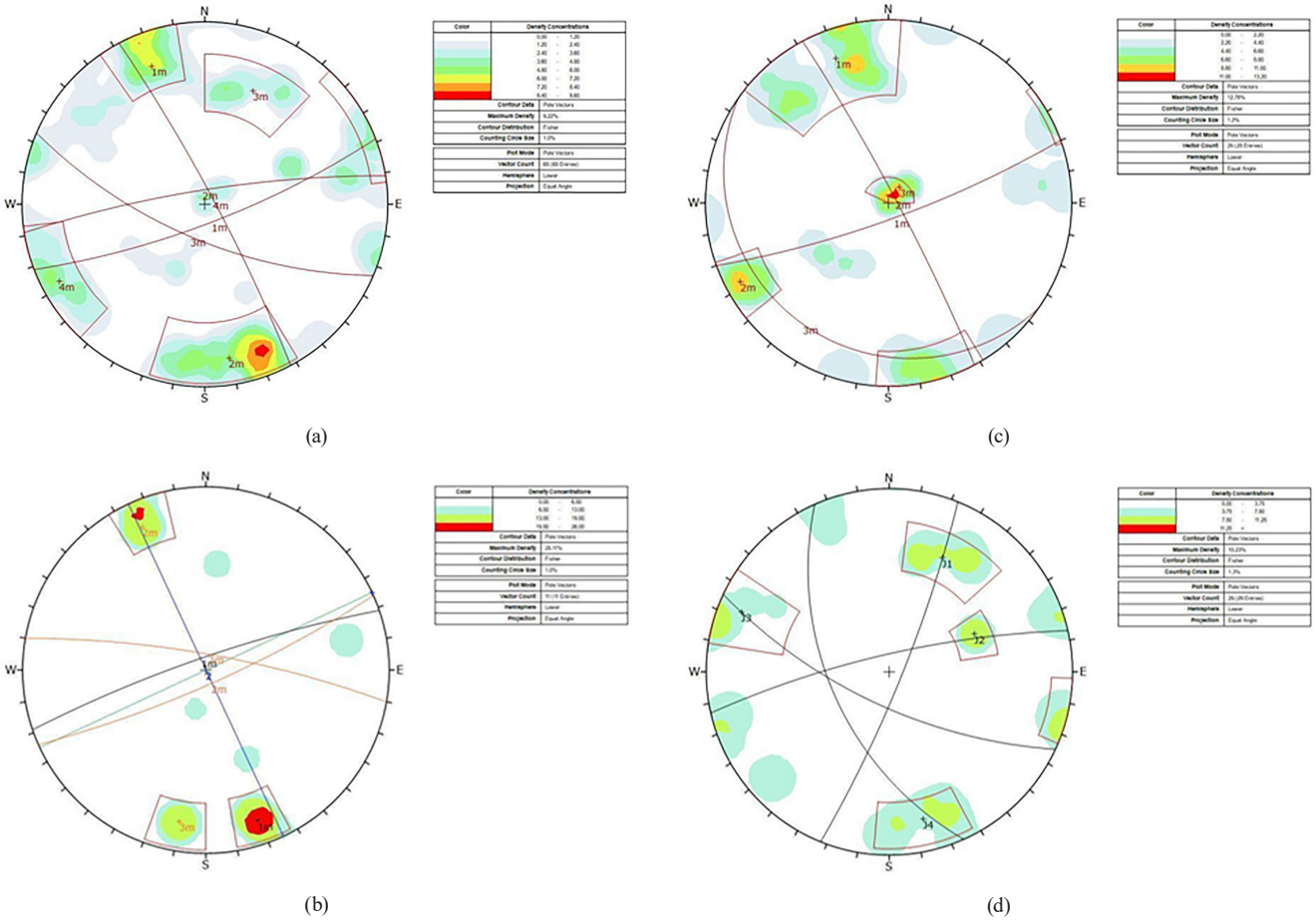

Fig. 11 Fracture and joint distribution on stereonet (a) All mapped fracture, (b) Burial chamber, (c) Rooms, (d) Sloping passage)

Table 5 Description of characteristic joint sets in engineering geological aspects

Parameters	Joint set 1	Joint set 2	Joint set 3	Joint set 4	Joint set 5
Dip/Dip direction	78/159	81/351	68/203	84/62	12/215
Average distance	0.30–0.60	0.2–0.6	0.5–2.0	0.1–0.3	n/a
Planarity	1 m/2 cm	1 m/5 cm	1 m/5 cm	1 m/5 cm	1 m/10 cm
Fracture length (m)	10	10	2–5	5–10	>10
Roughness	undulating-smooth	undulating-rough	undulating-smooth	planar-rough	undulating-smooth
Aperture	0.1–1	<0.1	0.1–1	0.1–1	<0.1
Infilling type	calcite	calcite	calcite	calcite	calcite
Infilling thickness	0.1–1	0.1–1	1–5	0.1–1	0.1–1

5.4 Schmidt hammer tests

The distribution of average uniaxial compressive strength values, which were retrieved from the rebound numbers evaluated by different positions of the tomb, is shown in Fig. 12. Based on the results, we can conclude that the scatter of values is low and average values are between 39–47 MPa. The lowest values originate from Room I and Room II sidewalls and columns and the highest value from Room II ceiling. Average values from the Sloping passage, Fore Chamber and Burial Chamber are very close to each other.

6 Discussion

6.1 Climatic conditions

The climatic conditions have an important role in the preservation of historic sites, and especially at heritage structures which were made of limestone. Hygric properties and the presence of selling clays can negatively influence the behavior of limestone [26]. Salts can also cause damage to the natural stone [27], and salt removal or consolidation of salt-loaded stones can be challenging [28]. Salt crystallization does not only occur on the surface, but subsurface galleries or underground tombs can also be damaged by salts [15]. The preservation of such surface structures requires detailed micro-climatic analyses [16]. Our study shows that the RH in the burial chamber is smaller than in the room or on the façade of the tomb (TT 25). It is coupled with a higher, nearly constant temperature in the chamber, which promotes salt crystallization. This is similar to the trend that was described from the underground archaeological-historical site of Yoshimi Hyaku Ana in Japan [15]. At the Japanese site, higher RH and lower temperatures were measured, and salt appearance showed a seasonality. The other difference is related to the differences in the host rock. At the study site a limestone is the host rock, while at Kofun tombs in Japan efflorescence of mixed soluble salts appears on highly porous volcanic tuff [15]. The studied tomb (TT 25) were cut in a less porous and apparently more durable limestone (Tharawan Chalk) than that of the ones of the Pyramids of Ghiza (Helwan Limestone) [26]. Nevertheless, salt accumulations were found in TT 25. Salts were uniquely observed in the deeper subsurface zones of the tomb (transition zone of the sloping passage and burial chamber) (Fig. 13), where the high moisture content of the

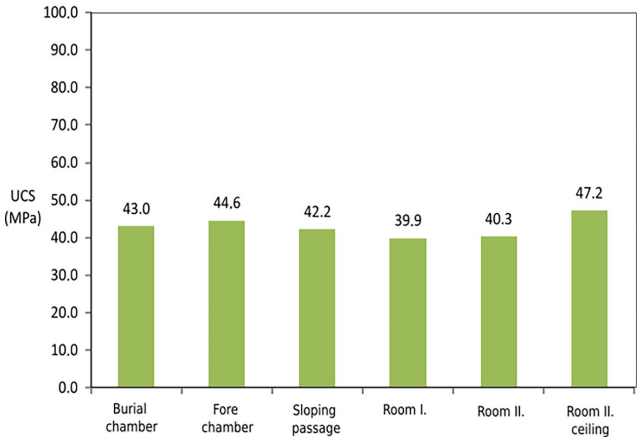

Fig. 12 UCS values according to Schmidt Hammer rebound

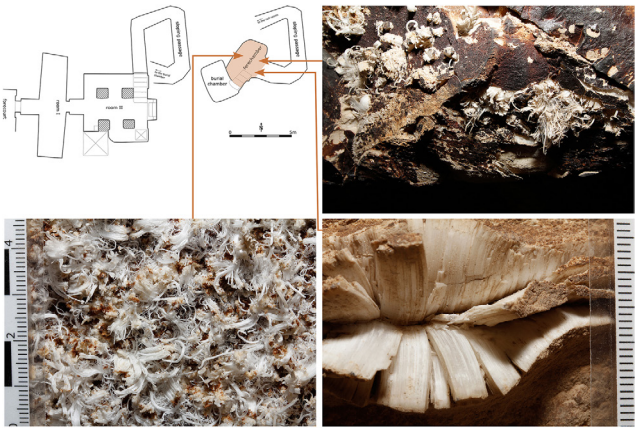

Fig. 13 Salt efflorescence in the fore-chamber

limestone walls was measured. The upper parts of the tomb do not show salt efflorescence since there are significant diurnal temperature changes (at the façade) or the changes in RH are fairly rapid (Table 4) and the moisture content of the walls are less (Fig. 10).

6.2 Rock mass classification

The fracture orientations in and around the burial chamber can be grouped into 4 major clusters, accompanied by a number of random joints. The distribution of joint orientations had a decisive influence on the orientation of the burial chamber. Joint set 1 and 2 are connected to the same strike but have different dip directions. Main direction of the tomb and wall surface were determined along these two joint sets, and these define the whole geometry inside. Joint sets 3 and 4 have different length, density properties. In addition, several random-type joints were measured and analyzed. In Room I and Room II bedding planes and stratification patterns can be observed also, with dip angles of 12 degrees (Table 5 Description of characteristic joint sets in engineering geological aspects). This data coincides with Dupuis et al. [14], who defined layer dip as < 10 degrees for the Asasif area near el-Khokha Hill and suggest a geology model where the Tarawan Chalk Formation is not part of the slipped formations of el-Khokha. This autochthon position and slipping-related deformation event can be the reason for steep joint sets and relatively high joint densities.

Walls and ceilings are probably stable because fractures and joints have favorable orientations and roughness parameters (Table 5). The joints contain predominantly thin (1–5 mm) thick fill material. The roughness of the fracture surfaces is smooth, mostly wavy or flat.

Based on these evaluations of host rock, rock mass classification can be carried out using Bieniawski's RMR method to properly assess the rock mass in rock mechanical aspects for further preservation works. Using results of Dips analyses, geotechnical mapping results presented in Table 5. and Schmidt Hammer tests (Fig. 12) RMR value can be calculated properly (Table 6).

The environment of the burial chamber can take values between RMR = 50–70. which means moderate and good rock environments. The relatively small span of excavation in the Rooms explains how they have remained stable for over 3000 years. It also relates to the Sloping passage, Fore Chamber and Burial Chambers with smaller inner diameters.

7 Conclusions

Four sub-vertical fracture systems were identified that are related to the structural geological evolution of the region, while one sub-horizontal joint system is related to the stratification of Tarawan Chalk. The fracture system negatively influences the stability of the tomb; however, a room collapse scenario is not feasible since the fracture orientation is favorable. The salt efflorescence was observed at the deeper part of the tomb (between the sloping passage and the burial chamber). This zone is characterized by higher and less variable temperatures and nearly constant relative humidity. The information from the results of climatic and engineering geological research provides valuable data for the conservation approach of TT 25. Strategies including structural reinforcement, environmental control, and site management should use this information. Protecting the rock tombs' stability and managing the microenvironment within them is crucial for their preservation. Further measures with the installed climate control systems and crack deformation measurements can help mitigate the impact of possible tourism and environmental fluctuations.

Acknowledgements

The financial support of the doctoral fellowship DKÖP-23 to Tamás Zomborácz (grant no. 2020-2.1.1-ED-2023-00239) is acknowledged. The fieldwork in the area would have been impossible without the support of the National Scientific Research Fund of Hungary (OTKA) and the research scholarship granted by Tempus Public Foundation. We are grateful for the help of Zoltán Imre Fábián, who is the field director of the Hungarian Archaeological Mission working in the area of TT 184 in Thebes.

Table 6 Rock mass classification result in RMR

RQD	UCS	Average spacing of discontinuities	Condition of discontinuities	Groundwater	Orientation	RMR
75–85	30–50 MPa	0.2–0.6	Slightly rough surfaces, separation is < 1, slightly weathered surfaces	Dry	Very favorable	RMR ratings
4	12	10	25	15	0	66

References

[1] Fuentes, J. M., Gallego, E., García, A. I., Ayuga, F. "New uses for old traditional farm buildings: The case of the underground wine cellars in Spain", Land Use Policy, 27(3), pp. 738–748, 2010. https://doi.org/10.1016/j.landusepol.2009.10.002

[2] Tinti, F., Barbaresi, A., Benni, S., Torreggiani, D., Bruno, R., Tassinari, P. "Experimental analysis of thermal interaction between wine cellar and underground", Energy and Buildings, 104, pp. 275–286, 2015. https://doi.org/10.1016/j.enbuild.2015.07.025

[3] Kleb, B. "Engineering-Geological Test on Settlements with Cellar Difficulties", Periodica Polytechnica Civil Engineering, 32(3–4), pp. 99–129, 1988.

[4] Zenah, J., Görög, P., Török, Á. "Stability of underground excavation in porous limestone: Influence of water content", Acta Montanistica Slovaca, 25(3), pp. 337–349, 2020. https://doi.org/10.46544/AMS.v25i3.7

[5] Zenah, J., Görög, P., Török, Á. "Historic subsurface dimension stone quarry and the stability of its galleries as a function of pillar width and thickness of cover bed", Environmental Earth Sciences, 81, 414, 2022. https://doi.org/10.1007/s12665-022-10539-x

[6] Kim, S. H., Lee, C. H., Jo, Y. H. "Behavioral characteristics and structural stability of the walls in the ancient Korean Royal Tombs from the sixth century Baekje Kingdom", Environmental Earth Sciences, 79, 81, 2020. https://doi.org/10.1007/s12665-020-8819-6

[7] Alcaíno-Olivares, R., Perras, M. A., Ziegler, M., Leith, K. "Thermo-mechanical cliff stability at tomb KV42 in the valley of the kings, Egypt", In: Sassa, K., Mikoš, M., Sassa, S., Bobrowsky, P. T., Takara, K., Dang, K. (eds), Understanding and reducing landslide disaster risk, Springer, Cham, 2021, pp. 471–478. ISBN 978-3-030-60196-6 https://doi.org/10.1007/978-3-030-60196-6_38

[8] Bardají, T., Martínez-Graña, A., Sánchez-Moral, S., Pethen, H., García-González, D., Cuezva, S., Cañaveras, J. C., Jiménez-Higueras, A. "Geomorphology of Dra Abu el-Naga (Egypt): The basis of the funerary sacred landscape", Journal of African Earth Sciences, 131, pp. 233–250, 2017. https://doi.org/10.1016/j.jafrearsci.2017.02.036

[9] Wolter, A., Ziegler, M., Colldeweih, R., Loprieno-Gnirs, A., Alcaino-Olivares, R., Perras, M. "Geological factors controlling evolution of theban tomb stability, Luxor", In: El-Qady, G. M., Margottini, C. (eds), Sustainable conservation of UNESCO and other heritage sites through proactive geosciences, Springer Geology, Springer, pp. 429–442. ISBN 978-3-031-13810-2 https://doi.org/10.1007/978-3-031-13810-2_23

[10] Ziegler, M., Colldeweih, R., Wolter, A., Loprieno-Gnirs, A. "Rock mass quality and preliminary analysis of the stability of ancient rock-cut Theban tombs at Sheikh 'Abd el-Qurna, Egypt", Bulletin of Engineering Geology and the Environment 78, pp. 6179–6205, 2019. https://doi.org/10.1007/s10064-019-01507-0

[11] Aubry, M.-P., Berggren, W. A., Dupuis, C., Ghaly, H., Ward, D. J., King, C., Knox, R. W., Ouda, K.-A. K., Youssef, M., Galal, W. F. "Pharaonic necrostratigraphy: a review of geological and archaeological studies in the Theban Necropolis, Luxor, West Bank, Egypt", Terra Nova, 21(4), pp. 237–256, 2009.

[12] Aubry, M.-P., Dupuis, C., Ghaly, H., King, C., Knox, R. W., Berggren, W. A., Karlshausen, C., Faris, M., Galal, W. F., Ouda, K. A.-K., Abdel-Sabour, A., Senosy, M., Soliman, M. F., Ward, D. J., Youssef, M. "Geological setting of the Theban Necropolis: implications for the preservation of the West Bank monuments", Orientalia Lovaniensia Analecta, PEETERS Publishers, 204, pp. 81–124, 2011.

[13] Aubry, M.-P., Dupuis, C., Berggren, W. A., Ghaly, H., Ward, D., King, C., Know, R. W. O'B., Ouda, K., Youssef, M. "The role of geoarcheology in the preservation and management of the Theban Necropolis, West Bank, Egypt", Proceedings of the Yorkshire Geological Society, 61(2), pp. 134–147, 2016. http://doi.org/10.1144/pygs2016-366

[14] Dupuis, C., Aubry, M.-P., King, C., Knox, R. W., Berggren, W. A., Youssef, M., Galal, W. F., Roche, M. "Genesis and geometry of tilted blocks in the Theban hills, near Luxor (upper Egypt)", Journal of African Earth Sciences, 61(3), pp. 245–267, 2011.

[15] Germinario, L., Oguchi, C. T. "Underground salt weathering of heritage stone: lithological and environmental constraints on the formation of sulfate efflorescences and crusts", Journal of Cultural Heritage, 49, pp. 85–93, 2021. https://doi.org/10.1016/j.culher.2021.02.011

[16] Xiong, J., Li, A., Liu, C., Dong, J., Yang, B., Cao, J., Ren, T. "Probing the historic thermal and humid environment in a 2000-year-old ancient underground tomb and enlightenment for cultural heritage protection and preventive conservation", Energy and Buildings, 251, 111388, 2021. https://doi.org/10.1016/j.enbuild.2021.111388

[17] Porter, B., Moss, R .L. B. "Topographical bibliography of ancient Egyptian hieroglyphic texts, reliefs, and paintings", I. The Theban Necropolis, Part 1: Private Tombs, The Clarendon Press, Oxford, UK, 1970.

[18] Kampp, F. "Die Thebanische Nekropole zum wandel des grabgedankens von der XVIII. bis zur XX. dynastie", (The Theban Necropolis: On the change in burial customs from the 18th to the 20th dynasty), Mainz am Rhein, 1996. ISBN 9783805315067 (in German)

[19] Fábián, Z. I. "Harper's Song Scene in the Tomb of Nefermenu (TT 184)", In: Specimina Nova XVI, Janus Pannonius University, pp. 1–13, 2002.

[20] Bieniawski, Z. T. "Engineering rock mass classifications", John Wiley and Sons, Inc, PA, 1989. ISBN 0471601721

[21] Barton, N., Choubey, V. "The shear strength of rock joints in theory and practice", Rock Mechanics, 10, pp. 1–54, 1977. https://doi.org/10.1007/BF01261801

[22] Barton, N. "Shear strength criteria for rock, rock joints, rockfill and rock masses: Problems and some solutions", Journal of Rock Mechanics and Geotechnical Engineering, 5(4), pp. 249–261, 2013. https://doi.org/10.1016/j.jrmge.2013.05.008

[23] Rocscience "Rocscience Inc. Dips, (8.025)" [computer program] Available at: https://www.rocscience.com/software/dips [Accessed: 01 March 2024]

[24] ISRM "Rock characterization testing and monitoring: ISRM suggested methods", ISRM, 1981. ISBN 978-0080273099

[25] ASTM "D 5873– 00 Standard test method for determination of rock hardness by Rebound Hammer Method", ASTM International, West Conshohocken, USA, 2005.

[26] Aly, N., Hamed, A., Abd El-Al, A. "The impact of hydric swelling on the mechanical behavior of Egyptian helwan limestone, Periodica Polytechnica Civil Engineering, 64(2), pp. 589–596, 2020. https://doi.org/10.3311/PPci.15360

[27] Khodabandeh, M. A., Rozgonyi-Boissinot, N. "The effect of salt weathering and water absorption on the ultrasonic pulse velocities of highly porous limestone", Periodica Polytechnica Civil Engineering, 66(2), pp. 627–639, 2022.

[28] da Fonseca, B. S., Pinto, A. P. F., Rucha, M., Alves, M. M., Montemor, M. F. "Damaging effects of salt crystallization on a porous limestone after consolidation treatments", Construction and Building Materials, 374, 130967, 2023. https://doi.org/10.1016/j.conbuildmat.2023.130967